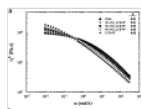
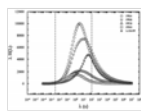
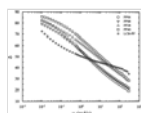
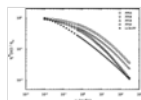


Table 1



Chemical Engineering Science

Volume 64, Issue 22, 16 November 2009, Pages 4719–4731

Morton Denn Festschrift



Rheological and thermal properties of blends of a long-chain branched polypropylene and different linear polypropylenes

Seyed H. Tabatabaei, Pierre J. Carreau, Abdellah Aji

CREPEC, Chemical Engineering Department, Ecole Polytechnique, C.P. 6079, Succ. Centre ville, Montreal, QC, H3C 3A7 Canada

Received 28 August 2008, Revised 2 April 2009, Accepted 3 April 2009, Available online 14 April 2009

[Show less](#)

doi:10.1016/j.ces.2009.04.009

[Get rights and content](#)

Abstract

Blends of a long-chain branched polypropylene (LCB-PP) and four linear polypropylenes (L-PP) having different molecular weights were prepared using a twin screw extruder. The linear viscoelastic properties suggested the immiscibility of the high molecular weight L-PP based blends, and the miscibility of the low molecular weight L-PP based blends. In addition, the Palierne emulsion model showed good predictions of the linear viscoelastic properties for both miscible and immiscible PP blends. However, as expected, the low-frequency results showed a clear effect of the interfacial tension on the elastic modulus of the blends for the high molecular weight L-PP based blends. A successful application of time–temperature superposition (TTS) was found for the blends and neat components. Uniaxial elongational properties were obtained using a SER unit mounted on an ARES rheometer. A significant strain hardening was observed for the neat LCB-PP as well as for all the blends. The influence of adding LCB-PP on the crystallinity, crystallization temperature, melting point, and rate of crystallization were studied using differential scanning calorimetry (DSC). It was found that the melting point and degree of crystallinity of the blends first increased by adding up to 20 wt% of the branched component but decreased by further addition. Adding a small amount of LCB-PP caused significant increase of the crystallization temperature while no dramatic changes were observed for blends containing 10 wt% LCB-PP and more. Furthermore, the crystalline morphology during and after crystallization of the various samples was monitored using polarized optical microscopy (POM). Compared to the neat linear polymers, finer and numerous spherulites were observed for the blends and LCB-PP. Dynamic mechanical (DMA) data of the blends and pure components were also analyzed and positive deviations from the Fox equation for the glass transition temperature, T_g , were observed for the blends.

Keywords

Polymers; Polypropylenes; Linear and branched polymer blends; Rheological properties; Thermal properties; Miscibility; Immiscibility

1. Introduction

Due to the higher melting point, lower density, higher chemical resistance, and better mechanical properties of polypropylene (PP) in comparison to polyethylene (PE), it is

widely employed for many industrial applications. However, the linear structure of L-PP limits its applications for processes where good extensional properties and melt strength are required such as thermoforming, film blowing, foaming and fiber spinning. On the other hand, it is well known that branched polymers have enhanced extensional properties and their blending with linear counterparts can improve their elongational behavior, particularly for PE (Aiji et al., 2003; Lohse et al., 2002; Steffl, 2004). With the recent development of branched PP, it is expected that the elongational properties of L-PP can be effectively enhanced when blended with a long-chain branched polypropylene (LCB-PP).

Long-chain branches are commonly introduced to linear PP via electron beam irradiation and post reactor chemical modification (Auhl et al., 2004; Tian et al., 2006a). Their effects on the processability have been reported in the literature (Gotsis et al., 2004; Stange and Münstedt, 2006). Gotsis et al. (2004) showed that branching up to an optimum level improved the processability in foaming and thermoforming processes, while further branching did not have a dramatic effect. Stange and Münstedt (2006) found that the strain hardening of branched polypropylenes caused not only a high melt strength, but also showed a significant homogeneity of deformation in the elongational experiments, which allowed forming foams with higher expansion ratios than L-PP.

In several cases (Aiji et al., 2003; Stange et al., 2005; McCallum et al., 2007; Fang et al., 2008), the rheological behavior of blends of linear and branched polypropylene and polyethylene has been investigated. It has been reported that branched polymers exhibit higher shear thinning, elasticity, and strain hardening compared to linear ones. Stange et al. (2005) showed that adding a small amount of LCB-PP significantly influences the rheological properties, especially the elongational behavior of linear PP blends. In addition, they found that the strain hardening of PP blends decreased as the strain rate increased while for the neat LCB-PP, enhancement of strain hardening was observed. McCallum and coworkers (2007) realized that the blending of branched and linear PP not only promoted the melt strength, but the mechanical properties increased as well. Aiji et al. (2003) showed that adding a small amount of low density polyethylene (LDPE) increased the strain hardening of linear low density polyethylene (LLDPE) resins. They also found that 10–20 wt% of LDPE is sufficient for improving the extensional property of LLDPE. Fang et al. (2008) concluded that an increase in the length of short branches and, possibly, the presence of a few long branches in metallocene LLDPEs and comparable molecular weights with LDPE could improve the miscibility of LLDPE/LDPE blends.

To our knowledge no work has been published regarding the effect of molecular weight of linear polypropylene on the rheological behavior of blends of linear and long-chain branched polypropylene. Using different rheological characterization methods, it will be shown that molecular weight has a crucial role on the miscibility of L-PP and LCB-PP. In addition, the influence of adding LCB-PP on the thermal properties, crystallization, and solid state behavior of the blends will be explored.

2. Experimental

2.1. Materials

Four commercial linear polypropylenes (PP40, PP28, PP08, and PP04) and a commercial branched polypropylene (LCB-PP) were selected. The PP28 and PP08 were supplied by ExxonMobil Company and had a melt flow rate (MFR) of 2.8 g/10 min (under ASTM conditions of \square and 2.16 kg) and 0.8 g/10 min, respectively, while the PP40, PP04, and LCB-PP were obtained from Basell Company and had a MFR of 4 g/10 min, 0.4 g/10 min, and 2.5 g/10 min, respectively. The main characteristics of the resins are shown in Table 1. The molecular weights of the L-PPs were evaluated from the relation between the zero-shear viscosity and the molecular weight (Fujiyama and Inata, 2002). The molecular weight distribution (MWD) was measured using a GPC (Viscotek model 350) with 1,2,4-Trichlorobenzene (TCB) as a solvent at a column temperature of 140 °C. The melting point, T_m , and the crystallization temperature, T_c , of the resins were obtained using differential scanning calorimetry. Blends containing 20, 40, and 60 wt%

LCB-PP were prepared using a twin screw extruder (Leistritz Model ZSE 18HP co-rotating twin screw extruder) followed by water cooling and pelletizing. The temperature profile along the barrel (from hopper to die) was set at 160/180/190/200/200/200/200 °C. The extrusion was carried out at 80 rpm. During blending, 3000 ppm of a stabilizer, Irganox B225, was added to avoid thermal degradation of the polymers. To make sure that all samples have the same thermal and mechanical history, unblended components were extruded under the same conditions.

Table 1.
Main characteristics of the neat polymers.

Resin code	Company	MFR (g/10 min)	Nomencl.	η_o^a (kPa s)	η_o^b (kPa s)		M_w/M_n	
Pro-fax 6523	Basell	4.0	PP40	9.8	9.8	501	2.8	159.8
PP4612	ExxonMobil	2.8	PP28	14.4	16.5	543	3.9	161.0
PP5341	ExxonMobil	0.8	PP08	43.6	49.5	772	2.7	160.0
Pro-fax 6823	Basell	0.4	PP04	58.3	67.5	812	4.3	159.6
Pro-fax 814	Basell	2.5	LCB-PP	18.6	19.5	N/A	2.3	158.4

a Zero-shear viscosity values obtained from the Carreau–Yasuda model, $T=190$ °C.

b Zero-shear viscosity values obtained from the area under the weighted relaxation spectrum curves, $T=190$ °C.

Table options

2.2. Rheological measurements

Dynamic melt rheological measurements were carried out using a Rheometric Scientific SR5000 stress controlled rheometer with parallel plate geometry (diameter of 25 mm and a gap of 1.5 mm). All measurements were carried out at [redacted] under nitrogen atmosphere to avoid thermal degradation. Molded discs of 2 mm thick and 25 mm in diameter were prepared using a hydraulic press at [redacted]. Time sweep tests were first performed at a frequency of 0.628 rad/s for 2 h. Material functions such as complex viscosity, elastic modulus, and weighted relaxation spectrum in the linear viscoelastic regime were determined in the frequency range from 0.01 to 500 rad/s. In order to obtain more accurate data, the frequency sweep test was carried out in four sequences while the amount of applied stress in each sequence was determined by a stress sweep test.

To measure the uniaxial elongational viscosity, an ARES rheometer equipped with a SER universal testing platform from Xpansion Instruments was used. The model used was SER-HV-A01, which is a dual windup extensional rheometer. It is capable of generating elongational rates up to [redacted]. Measurements were performed at [redacted] under nitrogen atmosphere.

2.3. Thermal analysis

Thermal properties of the various specimens were determined using a TA instrument differential scanning calorimeter (DSC) Q 1000. The samples were heated from 50 to [redacted] at a heating rate of [redacted] to eliminate initial thermal history, and then cooled to [redacted] at the same rate. The melting point and the degree of crystallinity were determined from the second heating ramp, also performed at a rate of [redacted]. Crystallinity values are reported, using a heat of fusion of 209 J/g for fully crystalline polypropylene (PP) (Arroyo and Lopez-Manchado, 1997).

2.4. Polarized optical microscopy (POM)

Crystallization monitoring was performed using polarized optical microscopy (OPTIHOT-2) to follow spherulites growth. For the non isothermal crystallization tests, films with a thickness of [redacted] were prepared using a twin screw extruder equipped with a slit die. The films were first heated on a programmable hot stage (Mettler FP82HT) from room

temperature to [REDACTED] at a heating rate of [REDACTED] and were kept at that temperature for 1 min to eliminate initial thermomechanical history, and then cooled to room temperature at the same rate.

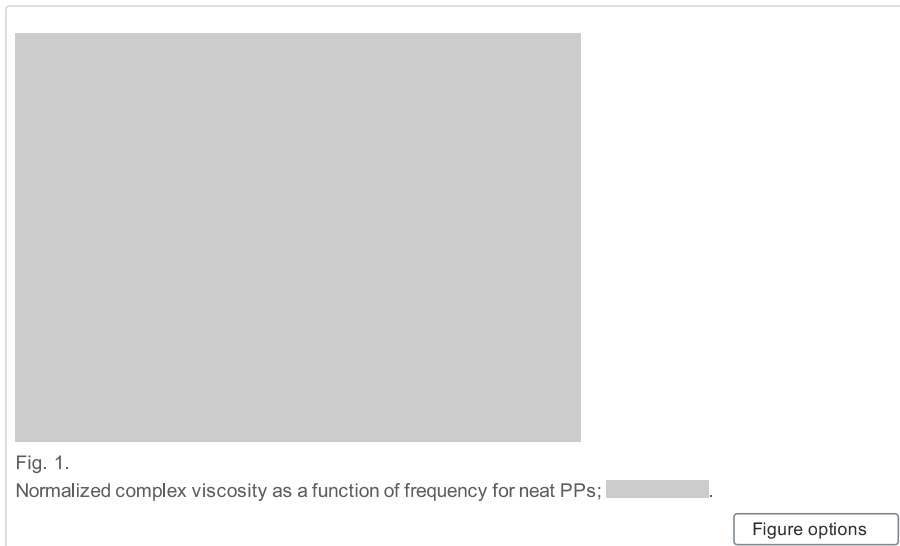
2.5. Dynamic mechanical analysis (DMA)

The solid state behavior of different samples was characterized using a TA instrument dynamic mechanical analyzer (DMA) 2980 inside an environmental test chamber (ETC). The temperature ranged from -40 to [REDACTED] at a rate of [REDACTED] and frequency of 1 Hz was applied to the rectangular shape samples. To generate low temperatures and to control temperature during heating, liquid nitrogen was used. The glass transition temperature was determined from the maximum of the G'' curves.

3. Results and discussion

3.1. Rheological characterization of the neat PPs

The complex shear viscosities normalized by the zero shear viscosities, obtained using the Carreau–Yasuda model (see Table 1), are plotted as a function of frequency for the neat PPs in Fig. 1. The LCB-PP exhibits a pronounced shear-thinning behavior due to the presence of long-chain branches. As the molecular weight of the L-PPs increases the behavior becomes more shear-thinning and the transition from the Newtonian plateau to the power-law region occurs at lower frequencies.



The plot of the loss angle, [REDACTED], as a function of frequency is shown in Fig. 2. A monotonic decrease in the loss angle is observed for the L-PPs while the LCB-PP shows an inflection in the curve with a tendency towards a plateau at high frequencies. Wood-Adams et al. (2000) related the magnitude and breath of the plateau to the weight fraction of branched chains. The larger elasticity of the LCB-PP compared to L-PPs at low frequencies is attributed to more entanglements due to the presence of long-chain branches. However, as the frequency increases, the number of entanglements decreases due to the more shear-thinning character of the branched PP (see Fig. 1).



Fig. 2.
Loss angle versus frequency for neat PPs; [redacted].

Figure options

To compare the relaxation behavior of the L-PPs and LCB-PP, the weighted relaxation spectra evaluated from dynamic moduli (G' , G'' , ω) using the NLREG (non linear regularization) software (Honerkamp and Weese, 1993) are plotted in Fig. 3 (the vertical dash lines represent the range of frequencies covered during the experiments). The area under the spectrum curve represents the zero-shear viscosity of the melt and it is reported in Table 1. A good agreement between these values and those obtained using the Carreau–Yasuda model is observed, suggesting that the relaxation spectra are accurate. It is obvious that the LCB-PP shows a longer relaxation time than the L-PPs, indicating that long-chain branches affect more the relaxation time than the larger molecules present in PP08 and PP04. The larger relaxation time for LCB-PP is attributed to changes in stress relaxation mechanisms. The simple reptation, as expected for linear polymers, no longer suffices to relieve stress when there are enough branches present and slower events such as arm retraction must occur.

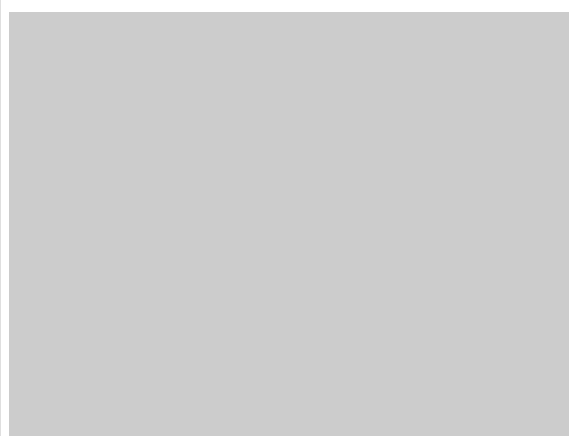


Fig. 3.
Weighted relaxation spectra for neat PPs; [redacted] (the vertical dash lines represent the range of frequencies covered during the experiments).

Figure options

3.2. Rheological characterization of the blends

The complex shear viscosities as a function of frequency for the PP40/LCB-PP and PP04/LCB-PP blends (two extreme cases) are shown in Figs. 4(a) and (b), respectively. It is clear that adding the LCB-PP causes a pronounced shear-thinning behavior due to the presence of long-chain branches (the power-index calculated for frequencies ranging from 0.1 to 10 rad/s is reported in the legend). In addition, it is obvious that the viscosities

of the PP40 based blends are intermediate between those of the neat components while those of the PP04 based blends are closer to that of the PP04. The behavior is typical of linear polymer melts and the complex viscosity of the blends follows the log additivity rule for low molecular weight based blends. This is shown in Figs. 5(a) and (b), where the complex viscosities at different frequencies are plotted as a function of the LCB-PP content. The logarithmic additivity rule is expressed as (Utracki and Schlund, 1987):

$$\log \eta^*(\omega) = \phi_{\beta} \log(\eta^*(\omega))_1 + (1 - \phi_{\beta}) \log(\eta^*(\omega))_2 \quad (1)$$

Turn on

where ϕ_{β} is the branched PP content in weight percent and η^* is the complex shear viscosity. The PP40 based blends obey the log additivity rule, as depicted in Fig. 5(a), suggesting miscibility of both PP components. However, significant deviations from this empirical relation are observed in Fig. 5(b) for the PP04 based blends in the entire composition range, suggesting that these two PP parts are immiscible. Deviations from the log mixing rule for blends of linear and branched PPs and PEs have been reported in the literature (Fang et al., 2008; Ho et al., 2002; Liu et al., 2002). It is believed that not only the amount of LCB-PP influences the miscibility of the blends, but also the molecular weights of both components as well as the branching structure (e.g. star-like or tree-like) of the LCB-PP are important factors affecting the miscibility.

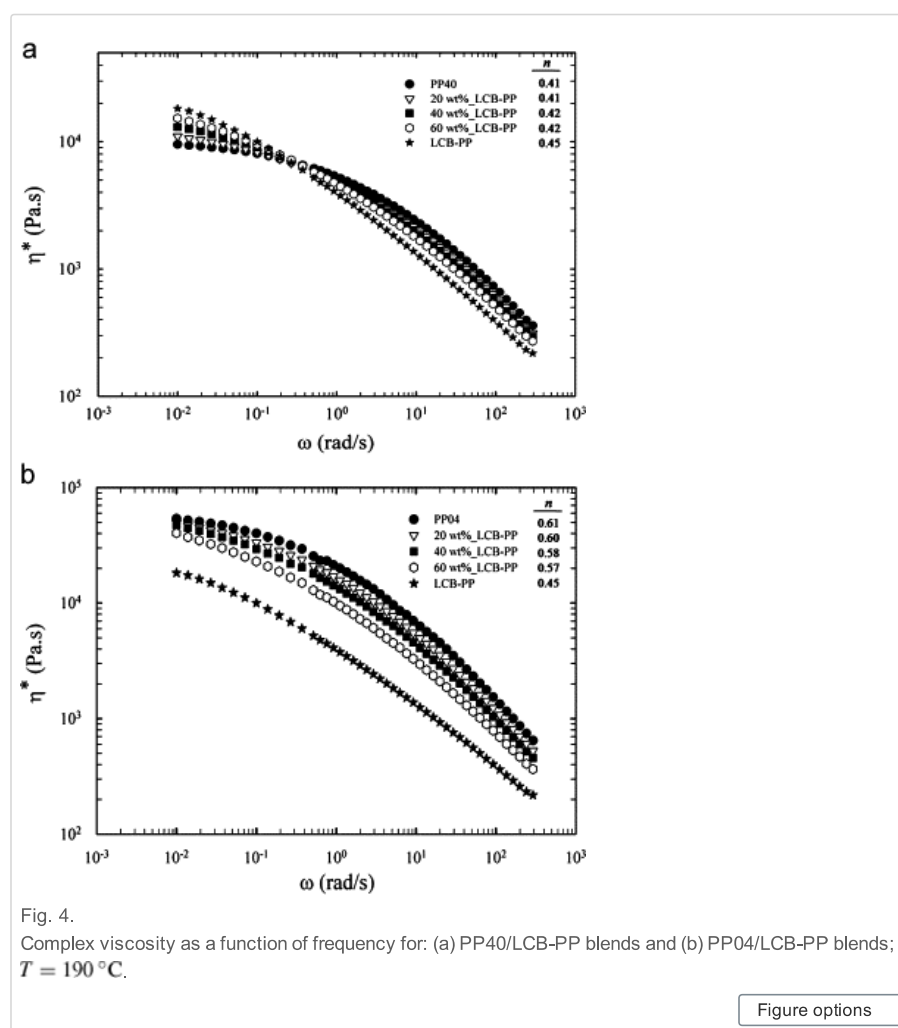


Fig. 4. Complex viscosity as a function of frequency for: (a) PP40/LCB-PP blends and (b) PP04/LCB-PP blends; $T = 190\text{ }^{\circ}\text{C}$.

Figure options

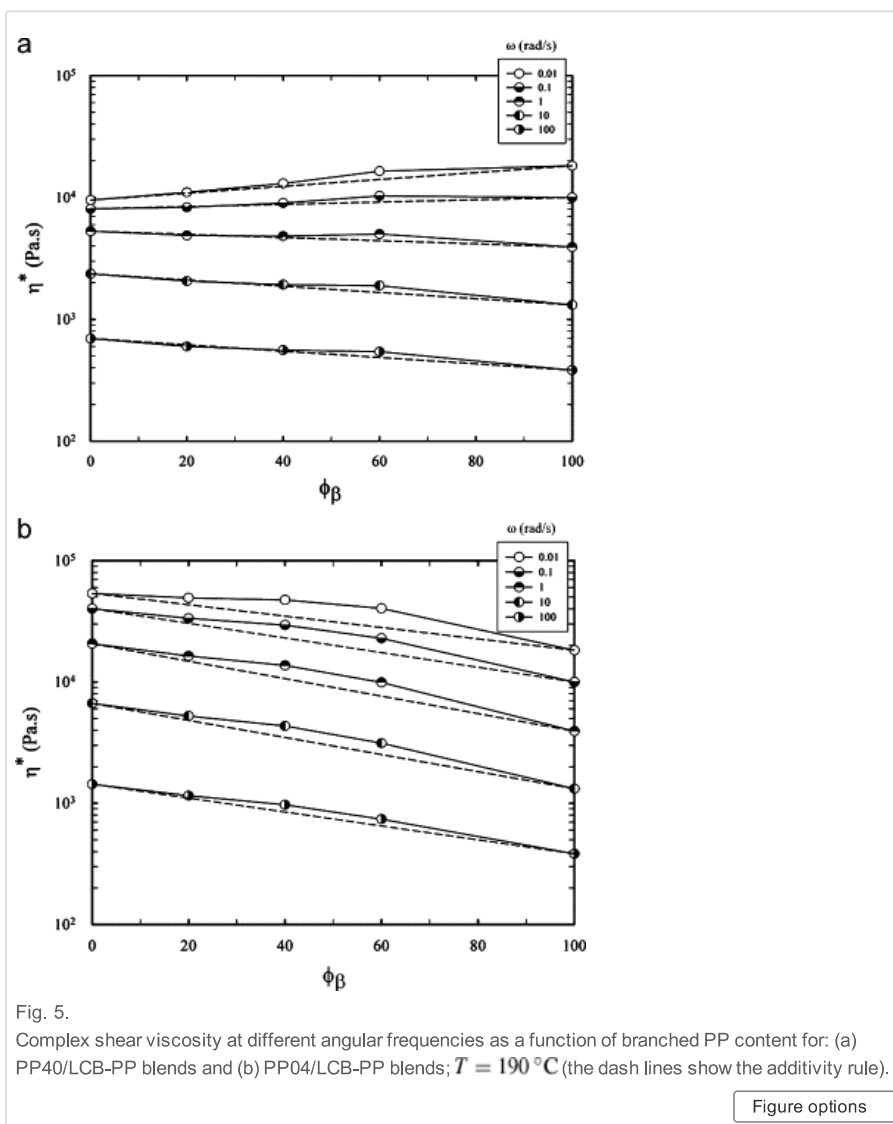


Fig. 5. Complex shear viscosity at different angular frequencies as a function of branched PP content for: (a) PP40/LCB-PP blends and (b) PP04/LCB-PP blends; $T = 190^\circ\text{C}$ (the dash lines show the additivity rule).

Figure options

The zero-shear viscosity obtained from the Carreau–Yasuda model is shown as a function of the LCB-PP content in Fig. 6. Good agreement with the log additivity rule for the blends having components with close melt flow indexes (i.e. PP40/LCB-PP and PP28/LCB-PP blends) is found, suggesting miscibility of the PP components. However, large deviations from the empirical rule are observed for the PP04/LCB-PP and PP08/LCB-PP blends, suggesting that the two components are immiscible. It should be noted that at low frequencies (Newtonian region), a large increase in the number of entanglements due to the LCB-PP addition is expected for all the samples. Therefore, it is unlikely that the deviations from the log mixing rule could be explained for the PP04/LCB-PP and PP08/LCB-PP blends only.




Fig. 6.
Zero-shear viscosity as a function of LCB-PP content;  (the dash lines show the additivity rule).

Figure options

To see the effect of molecular weight of L-PP on the relaxation behavior of the blends, the weighted relaxation spectra of the PP40/LCB-PP and PP04/LCB-PP blends are illustrated in Figs. 7(a) and (b), respectively. The addition of LCB-PP changes the relaxation mechanism from simple reptation to arm retraction, which retards the movement of chains along their backbone; hence, the maxima in the curves shift to longer times and the spectrum shape becomes broader. Note that for the PP40/LCB-PP blends, the positions of the peaks are intermediate to those of the neat components, indicating again miscibility, while for the PP04/LCB-PP blends non uniform changes in the peaks are observed.

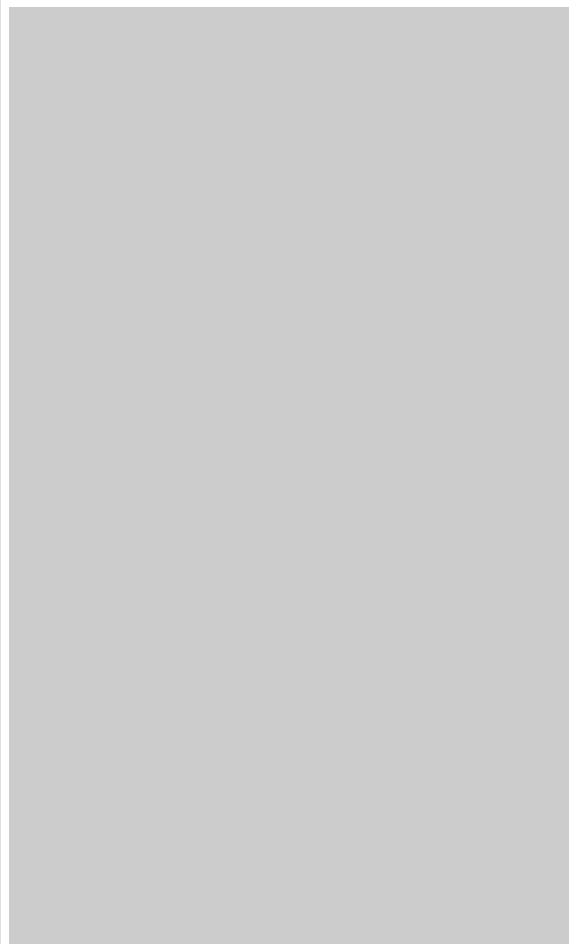


Fig. 7.


Weighted relaxation spectrum for: (a) PP40/LCB-PP blends and (b) PP04/LCB-PP blends;  (the vertical dash lines represent the range of frequencies covered during the experiments).

Figure options

The behavior can also be analyzed using Cole–Cole plots of η'' versus η' , as illustrated in Fig. 8. The semicircular shape for the PP40/LCB-PP blends (Fig. 8(a)) is another evidence of miscibility (Kwang et al., 2000; Utracki, 1991), while some synergistic effects for the PP04/LCB-PP blends (Fig. 8(b)) are observed. It should be noted that the curves of the high M_w based blends are closer to that of the neat L-PP component, which confirms the results demonstrated in Fig. 4.

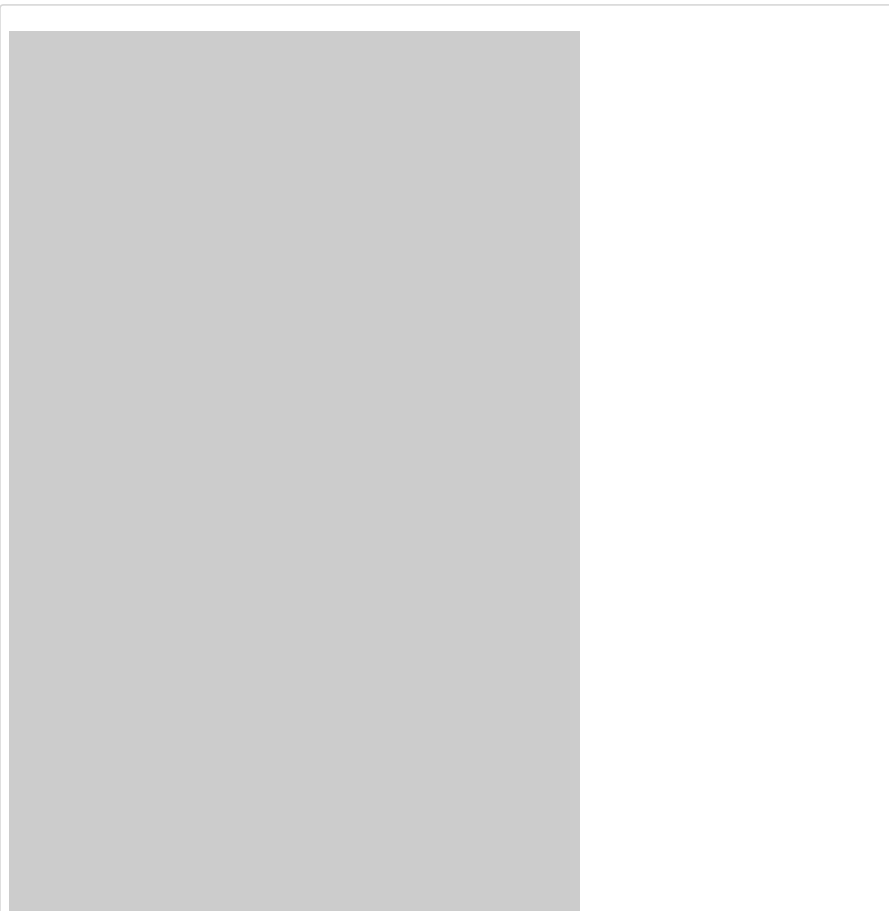



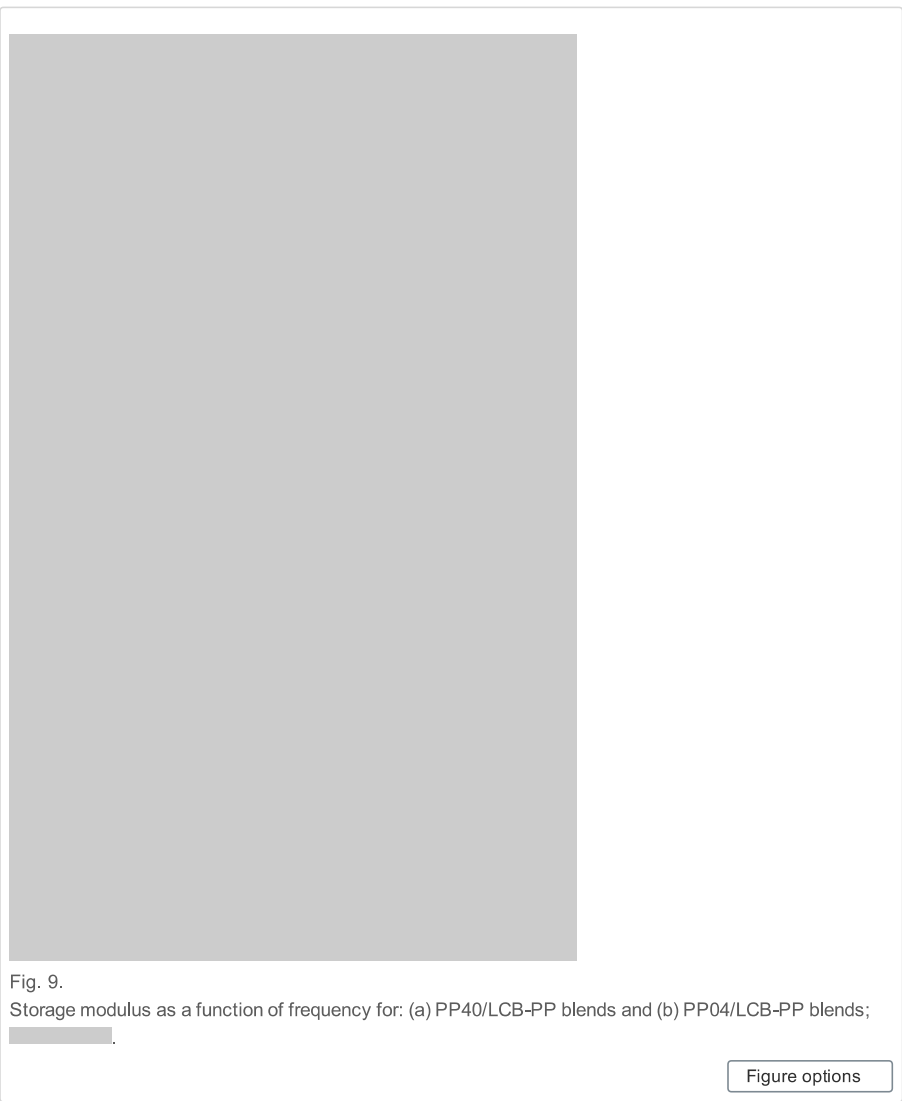
Fig. 8. Cole–Cole plots for: (a) PP40/LCB-PP blends and (b) PP04/LCB-PP blends; .

Figure options

Figs. 9(a) and (b) illustrate the storage modulus of the PP40/LCB-PP and PP04/LCB-PP blends, respectively. For the PP40 based blends, at low frequencies, the storage modulus of the LCB-PP is larger while the effect becomes inverted at high frequencies. For the blends containing a high molecular weight component (Fig. 9(b)) some synergistic effects at low frequencies are seen for all compositions, which is possibly due to the immiscibility of these blends. The increase of elasticity at low frequencies is common in immiscible blends and has been interpreted in the context of emulsion models (Chun et al., 2000; Palierne, 1990; Utracki, 1991).



Palierne (1990) developed a model to predict the linear viscoelastic properties of immiscible emulsion-type blends. For a narrow distribution of droplet diameters (Bousmina and Muller, 1993) and constant interfacial tension, the complex modulus of the blend is expressed by:

$$\text{[Redacted Equation]}$$

where H^* is defined as:

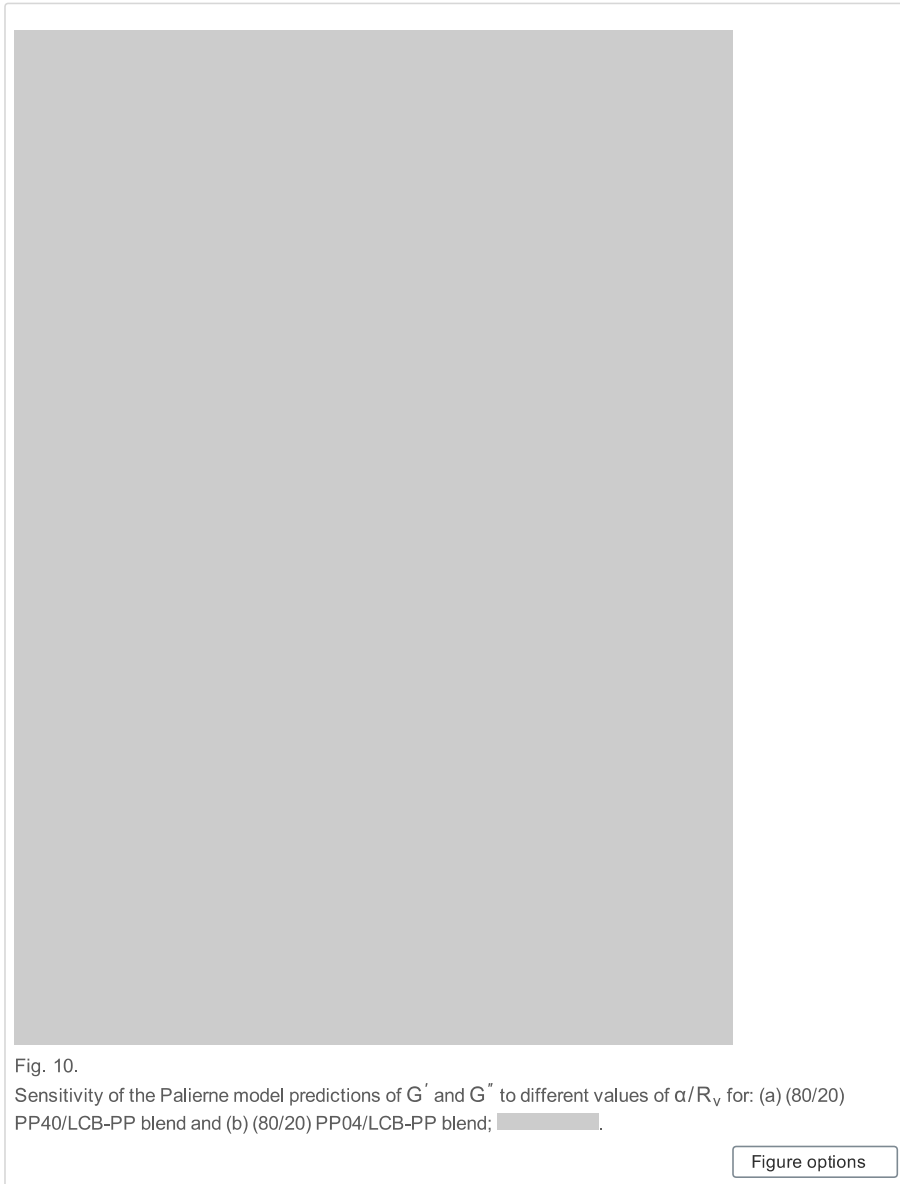
$$\text{[Redacted Equation]}$$

where ϕ is the volume fraction of the droplets of volume average radius R_v , α is the interfacial tension, and G_m and G_d are the complex moduli of the matrix and droplets, respectively.

Due to the low optical contrast between the PP components it was impossible to obtain the dimensions of drops in the PP blends and hence R_v . Following Fang et al. (2005) and Hussein and Williams, 2001 and Hussein and Williams, 2004, α/R_v was used as a single parameter to find the best fits of the experimental data for the blends containing 20 wt% LCB-PP with low and high molecular weight L-PP components.

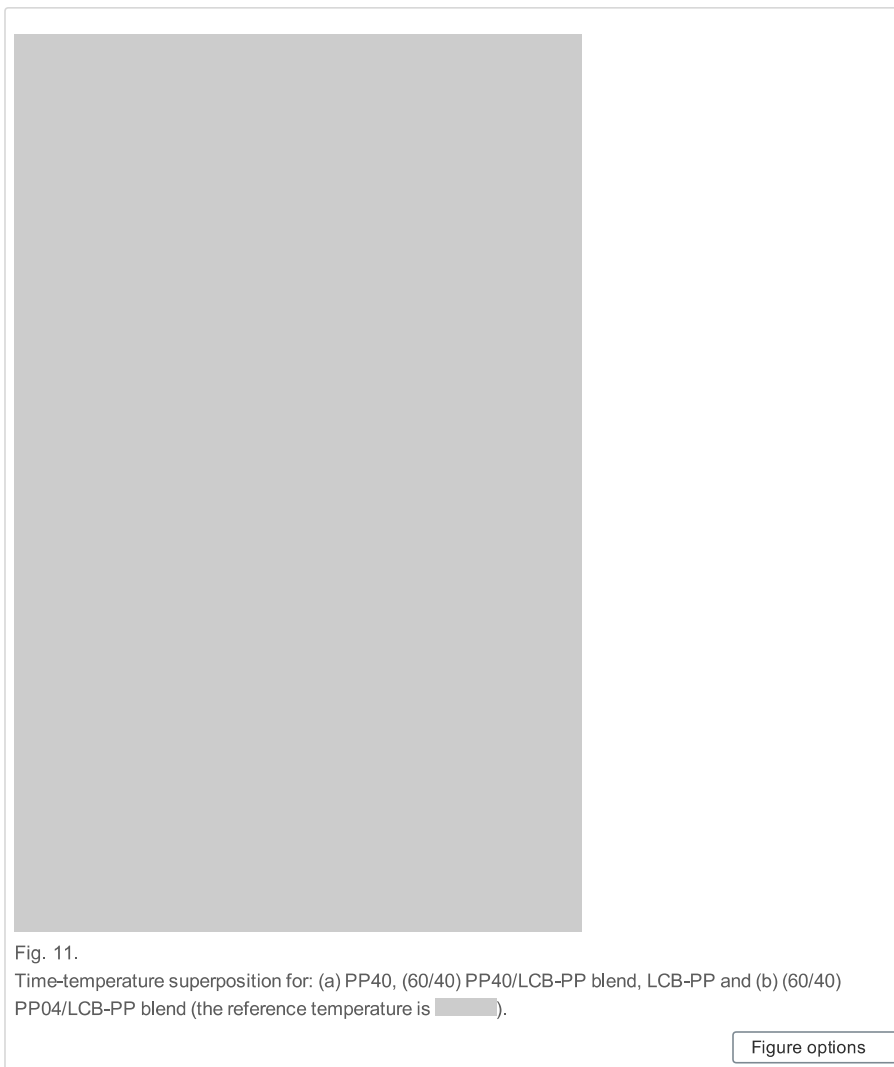
Figs. 10(a) and (b) demonstrate the influence of α/R_v (0, 100, and 500) on the storage and loss moduli predicted by the Palierne model for the (80/20) PP40/LCB-PP and (80/20) PP04/LCB-PP, respectively. It is obvious that the G' values predicted by the

model are not sensitive to the value of α/R_v and are in good agreement with the experimental data. In contrast, the G' values are dramatically influenced by the value of α/R_v at low frequencies. For the (80/20) PP40/LCB-PP blend the best fit of the model with the experimental data was achieved for $\alpha/R_v=0$ while for (80/20) PP04/LCB-PP blend, the best fit was obtained for $\alpha/R_v=100$. A value of the interfacial tension equal to 0 for the (80/20) PP40/LCB-PP blend is indicative of miscibility. However, the non zero value of α/R_v for the (80/20) PP04/LCB-PP blend is indicative of the presence of a dispersed phase. Assuming an interfacial tension of 0.1 mN/m for the PP pair (PP04/LCB-PP), the corresponding droplet radius is estimated to be around [REDACTED]. Hence, the hypothesis of immiscibility for these blend components is reasonable.



The role of adding the long-chain branched component on the temperature sensitivity of complex viscosity of the blends is examined via the time–temperature superposition (TTS) principle. The results for the unblended polymers as well as for two blends are depicted in Figs. 11(a) and (b), respectively (to facilitate the comparison between data, the curves have been shifted by a multiplication factor as indicated). The shift factor, a_T , was obtained from the temperature dependency of the zero-shear viscosity and was larger for the branched polymer compared to the linear one. From Fig. 11, it is clear that TTS holds for all the samples. van Gorp and Palmen (1998) proposed a refined analysis to check the validity of the TTS principle. The TTS principle is respected when the plot of the loss angle, [REDACTED], as a function of complex modulus, $G^* = (G'^2 + G''^2)^{1/2}$,

superimpose in a single curve for all temperatures. The analysis of [van Gorp and Palmen \(1998\)](#) was examined for (60/40) PP40/LCB-PP and (60/40) PP04/LCB-PP blends as well as their neat components (the results are not shown). A single curve for each sample for various temperatures was observed, indicating that the TTS principle holds for all the samples. [Macaubas and Demarquette \(2002\)](#) investigated the applicability of TTS for a blend containing 10 wt% PP in PS and a blend containing 10 wt% PP in HDPE using the van Gorp-Palmen analysis. The immiscible 10 wt% PP/HDPE blend was observed to respect the principle, but not the immiscible 10 wt% PP/PS blend. This was explained by large differences of the flow activation energy, horizontal shift factor, and of the interfacial tension for PP and PS compared to those of PP and HDPE. In our case, although different rheological characterization methods suggested immiscibility of the PP04/LCB-PP blend systems, no significant differences for the flow activation energy and the shift factor were found for the blend components. In addition, a small value of interfacial tension between the components is expected. Hence, these observations can explain the validity of TTS for the (60/40) PP04/LCB-PP blend.



In contrast to oscillatory shear data, uniaxial extension is very sensitive to molecular and microstructural parameters ([Münstedt et al., 1998](#); [Wagner et al., 2000](#)). The transient elongational viscosity of the resins and blends at different strain rates and is illustrated in [Fig. 12](#) (as in [Fig. 11](#), the curves have been shifted by a multiplication). As expected, the linear polypropylenes respect the linear viscoelastic behavior over a large strain range where the transient elongational viscosity is equal to three times that the transient viscosity in simple shear determined using the relaxation spectrum according to the following equation:

(4)

To obtain the transient elongational viscosity from the above equation 100 modes (N) were used.



Fig. 12. Transient elongational viscosities as a function of time at different Hencky strain rates, $\dot{\gamma}$, for: (a) PP40/LCB-PP blends and (b) PP04/LCB-PP blends; \square (the solid lines represent the linear behavior calculated from the relaxation time spectrum).

Figure options

A significant strain hardening is observed for the LCB-PP as well as for all the blends. A sharper increase in the extensional viscosity curves and deviations from the linear viscoelasticity at shorter times were found as the weight fraction of the LCB-PP increases from 0.20 to 1. [Stange et al. \(2005\)](#) found that adding a small amount of the same long-chain branched PP to a linear PP (different than those used in this work) caused strain-hardening and the effect was attributed to long-chain branching. Similar results for blends of LDPE and LLDPE were reported by [Ajji et al. \(2003\)](#) and [Wagner et al. \(2004\)](#). Note that for the PP04/LCB-PP blends at all strain rates the shape of the curves are similar to that of the PP04, in accordance with the shear data (see [Fig. 4](#) and [Fig. 8](#)), which is probably due to immiscibility of these blends. As for the shear properties, it is clear that the elongational properties are dominated by the high molecular weight component.

The behavior of the PP28/LCB-PP blends was similar to that of the PP40/LCB-PP blends and that of the PP08/LCB-PP was close to the PP04/LCB-PP. For the sake of simplicity and brevity, the results for the PP28/LCB and PP08/LCB blends are not shown.

3.3. Thermal characterization

In the melting curve of the neat L-PPs, a small peak around [redacted] was observed and attributed to the presence of a small amount of beta (β) or hexagonal crystalline form of PP (Jang et al., 2001). The magnitude of the peak was reduced when up to 5 wt% of the branched PP was added and disappeared by further addition of the LCB-PP. As the peak was not seen for the neat LCB-PP, it could be concluded that the presence of long-chain branches prevented the formation of beta crystals. Tian et al. (2006b) studied the crystalline structures of linear and long chain branched PPs using wide-angle X-ray diffraction (WAXD). They found that linear PPs could crystallize in the α and β forms, while branched PPs crystallized only in the α crystalline form, in agreement with our DSC results.

Melting and crystallization temperatures obtained from the peak positions as well as the degree of crystallinity of the various materials and blends are presented in Table 2. The melting point of the blends first increases by adding 20 wt% LCB-PP to the linear PPs while further addition reduces it. The reason for this behavior is unclear at present and different trends for the melting point of blends of linear and branched PPs have been reported in the literature (McCallum et al., 2007). Generally, a single melting peak was observed for all the blends. However, as the melting points of the components are very close, this cannot be considered as an indication of miscibility.

Table 2.

Melting point (T_m), crystallization temperature (T_c), and degree of crystallinity (X_c) of the neat PPs as well as the blends (\pm indicates the standard deviation of the crystallinity).

Sample	[redacted]	[redacted]	X_c	Sample	[redacted]	[redacted]	X_c
PP04	159.6	116.9	36.8 \pm 1.1	PP28	161.0	114.4	40.0 \pm 0.9
(20/80) PP04/LCB-PP	161.9	125.5	41.6 \pm 0.7	(20/80) PP28/LCB-PP	162.1	126.5	42.2 \pm 1.4
(40/60) PP04/LCB-PP	161.7	126.4	37.5 \pm 0.5	(40/60) PP28/LCB-PP	161.6	127.5	41.3 \pm 0.7
(60/40) PP04/LCB-PP	160.5	127.1	36.9 \pm 1.2	(60/40) PP28/LCB-PP	160.6	127.7	35.6 \pm 1.1
LCB-PP	158.6	128.4	35.0 \pm 1.0	LCB-PP	158.6	128.4	35.0 \pm 0.9
PP08	160.0	117.3	37.8 \pm 1.5	PP40	159.8	119.2	38.8 \pm 1.9
(20/80) PP08/LCB-PP	161.5	126.0	40.2 \pm 0.8	(20/80) PP40/LCB-PP	161.3	126.9	40.8 \pm 1.1
(40/60) PP08/LCB-PP	160.5	127.3	39.6 \pm 0.8	(40/60) PP40/LCB-PP	160.9	127.5	40.2 \pm 0.7
(60/40) PP08/LCB-PP	160.2	127.6	39.1 \pm 0.3	(60/40) PP40/LCB-PP	160.0	127.8	37.3 \pm 1.2
LCB-PP	158.6	128.4	35.0 \pm 1.0	LCB-PP	158.6	128.4	35.0 \pm 0.9

Table options

Adding LCB-PP to the linear PPs causes a significant increase in the crystallization temperature, T_c , for all LCB contents, with the maximum change occurring at 20 wt% LCB-PP (see Table 2). Similar observations for blends of other linear and branched PPs were reported by McCallum et al. (2007). To determine at which concentration the transition for the crystallization temperature occurs, additional blends containing 2, 5, and 10 wt% LCB-PP were prepared and analyzed and the results are shown in Fig. 13. It is clear that T_c of PP28 changes from 114.4 to 123.3 °C after adding only 2 wt% LCB-PP while further addition of LCB-PP causes a slight increase of the crystallization temperature. Dramatic increases in the crystallization temperature have also been reported in literature (Zhang et al., 2007) when a nucleating agent was added to a neat polymer. It was interpreted by a lower free energy for the heterogeneous nucleus formation compared to that of the homogeneous nucleus formation. In our case, one possibility for the dramatic rise of T_c can be explained by a large increase of the heterogeneous nuclei sites due to addition of the long-chain branches. However, the residual catalysts used to produce the long-chain branches may also act as nucleating agents, which could be another reason for the increase of T_c .



Fig. 13.

DSC cooling thermographs for PP28, LCB-PP, and their blends at [redacted].

Figure options

Table 2 also reports the results of crystallinity measurements for all the blends and for all concentrations. A significant increase of the degree of crystallinity is observed when 20 wt% of LCB-PP is added to the L-PPs, and this for all the blends. It was also found that the transition in this crystallinity increase occurs upon the addition of only 2 wt% LCB-PP (the data are not presented here). It is postulated that a small amount of the LCB-PP increases the number of nuclei sites, resulting in an increase of crystallinity. On the one hand, further addition of the branched polymer increases the number of nuclei sites, on the other hand, the branches prevent chain mobility, leading to a decrease in crystallinity when more than 20 wt% LCB-PP is added.

To examine the effect of adding LCB-PP on the rate of crystallization, the relative crystallinity (obtained from the area under the exotherm peak of the crystallization curve) as a function of time for the PP28/LCB-PP blends was determined and the results are shown in Fig. 14. The relation between time, t , temperature, T , and cooling rate, Φ , is expressed as (Tian et al., 2007):

$$[redacted] \quad (5)$$

where T_o is the onset crystallization temperature. All the curves show an S shape, similar for all the components and blends, as seen in Fig. 14. However, a lower transition appeared at the later crystallization stage for samples containing the LCB-PP. In general, the rate of crystallization is first controlled by nucleation and then by growth of crystals and packing (Tian et al, 2007). As mentioned above, adding a branched polymer to a linear one increases the number of nuclei sites resulting in a larger crystallization rate for the blends in the early stages of the crystallization. However, due to more impingements of the crystalline parts, crystalline growth is stopped at later stages. Tian et al. (2007) studied the crystallization kinetics of a linear PP and PPs containing different levels of long chain branching (LCB). Similar to our results, their finding showed that the presence of LCB accelerated crystallization at the early stage, and then the reverse effect on crystallization was observed at the later stage. The half-time of crystallization, $t_{1/2}$, can be obtained from Fig. 14. It is obvious that the value of $t_{1/2}$ decreases as the level of the LCB-PP increases, indicating that the presence of the LCB-PP accelerates the crystallization behavior of the L-PP. It is speculated that the branches have the role of heterogeneous nucleating sites, which was also mentioned by Tian et al. (2007).



Fig. 14.
Curves of relative crystallinity versus time for the PP28/LCB-PP blends.

Figure options

The Avrami equation can be used to elucidate the differences in the primary nucleation for the blend systems (Agarwal et al., 2003). It is expressed as:

$$1-X(t)=e^{-kt^n} \quad (6)$$

where $X(t)$ is the amount of crystallinity and n and k are the Avrami constants. The exponent n depends on the nucleation type and growth geometry (Agarwal et al., 2003): n values close to 1, 2, and 3 correspond to a rod, disk, and sphere like growth geometry, respectively (Agarwal et al., 2003). The double logarithm of the above equation leads to:

$$\log[-\ln(1-X)] = \log k - n \log t \quad (7)$$

Plots of $\log[-\ln(1-X)]$ versus $\log t$ are illustrated in Fig. 15. To facilitate the comparison between data, the non-linear portion of the curves was removed. The value of the Avrami exponent, shown in the figure, is close to three indicating sphere like growth of the crystalline phase for all the samples. The value of n changes upon adding LCB-PP to the blends. This suggests different nucleation and growth mechanisms for the samples containing LCB-PP.

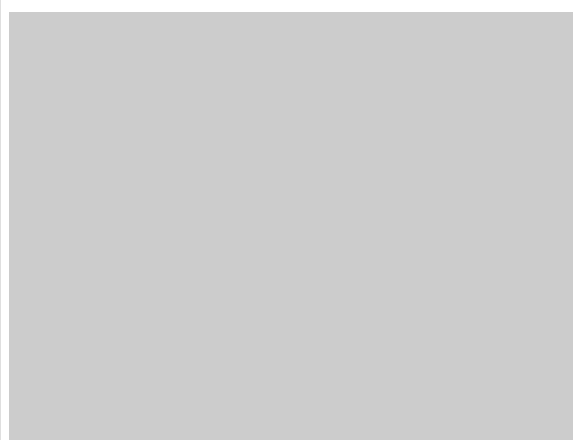


Fig. 15.
Plots of $\log[-\ln(1-X(t))]$ as function of $\log(t)$ for PP28, LCB-PP and the 40 wt% PP28/LCB-PP blend.

Figure options

The crystal morphology of the PP28, LCB-PP, and the blends containing 2 and 20 wt % LCB-PP were observed using POM, and presented in Fig. 16. Large spherulites, as expected for linear polymers, are observed for PP28 (Fig. 16(a)). The number of

spherulites increased noticeably and their size decreased by adding only 2 wt% LCB-PP (Fig. 16(b)), indicating that more nucleating sites have been created. The crystal structures of the (80/20) PP28/LCB-PP blend was similar to that of (98/2) PP28/LCB-PP and the neat LCB-PP showed slightly smaller spherulites. The optical microscopy revealed that the spherulite growth in PP28 was due to sporadic nucleation, while that of the branched PP containing blends is attributed to an instantaneous nucleation. Sporadic nucleation happens by chain aggregation, which needs a longer time, whereas heterogeneous nucleation happens as soon as the temperature reaches the crystallization temperature (Guan et al., 2003; Tian et al., 2007). This can explain the results presented in Fig. 14.

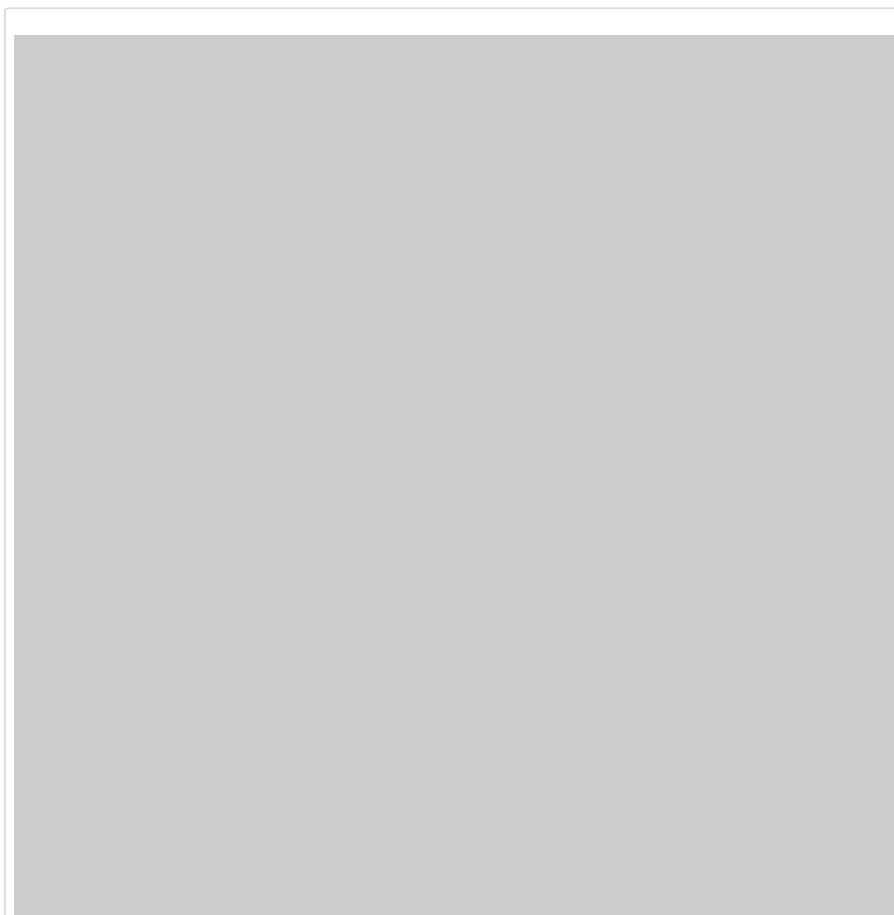


Fig. 16.

Optical micrographs at the end of crystallization for samples non isothermally crystallized at [redacted] from the melt: (a) PP28, (b) (98/2) PP28/LCB-PP, (c) (80/20) PP28/LCB-PP, and (d) LCB-PP.

Figure options

As mentioned before, it is believed that the residual catalyst in the branched samples act as a nucleating agent. In order to separate the contribution of the residual catalyst from that of long-chain branches on the final morphology, 0.2, 0.5, and 1 wt % sodium benzoate (SB) (supplied by LAB MAT), in the form of powder, were dry blended with the PP28. From Dong et al., (2008) and Zhu et al., (2006), it is known that SB acts as an α form nucleating agent. Fig. 17 illustrates optical micrographs of the PP28 and nucleated samples as well. Obviously, the reduction of the spherulite size is observed when the nucleating agent is added to the linear polymer. These observations accompanied with those presented in Fig. 16 suggest a significant coupling effect between residual catalysts and long chain branches, which yields to the presence of large number of very small spherulites for the specimens containing the branched polymer.

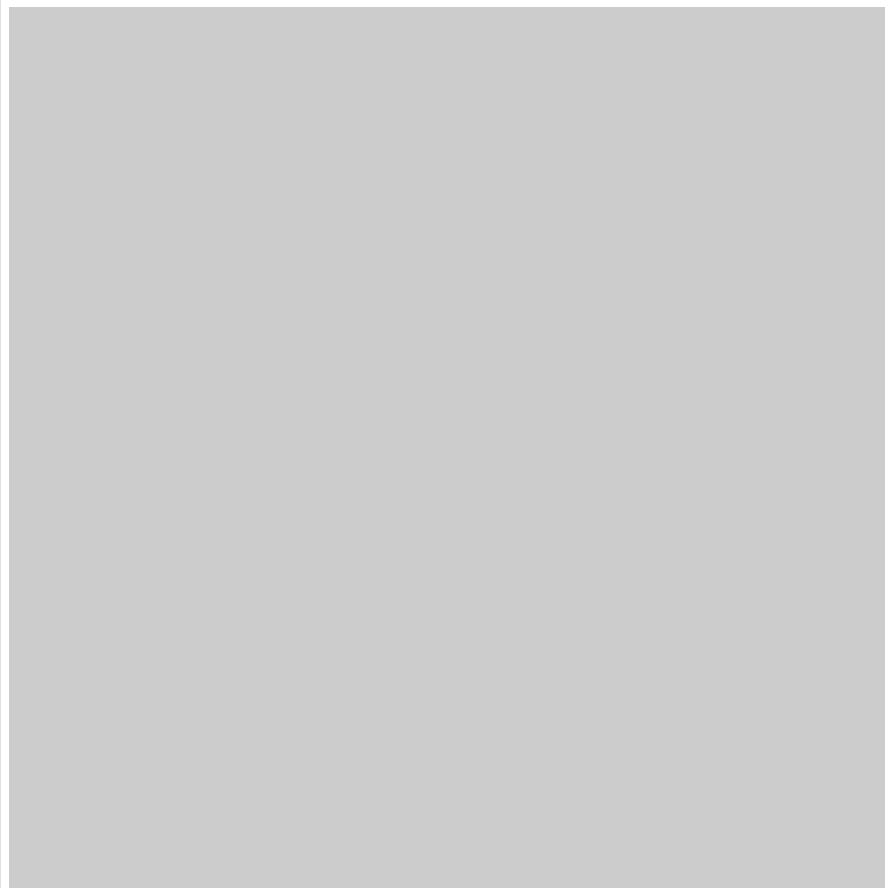


Fig. 17.
Optical micrographs at the end of crystallization for samples non isothermally crystallized at [redacted] from the melt. (a) PP28, (b) 0.2 wt% nucleated, (c) 0.5 wt% nucleated, and (d) 1 wt% nucleated.

Figure options

3.4. Solid state properties

The glass transition temperature of samples, obtained from the position of the maximum in the G'' curves, is presented in Fig. 18. The solid lines were sketched accordance to the Fox equation:

$$[redacted] \quad (8)$$

where T_{g1} and T_{g2} are the glass transition temperature of the unblended samples and w is the weight fraction of the branched component. The Fox equation can describe the T_g of polymer blends when no strong interaction exists between the polymer components (Boileau et al., 2001). In other words, significant deviations from this empirical relation for the polymer systems involving strong forces (e.g. hydrogen bonding) have been reported (Boileau et al., 2001). In our case, a positive deviation, with maximum occurring at 20 wt% of the branched PP, from the Fox equation is observed (Fig. 18).



Fig. 18.
Glass transition temperature as a function of LCB-PP content (the solid lines represent the Fox equation).

Figure options

4. Conclusions

In this study, the rheological, crystallization, and thermal properties of blends of different molecular weight linear polypropylenes (L-PP) and a long-chain branched polypropylene (LCB-PP) were investigated. It was found that the shear and extensional properties of the blends were dominated by the L-PP for blends containing high molecular weight component. Based on the log-additivity rule for the zero-shear viscosity, Cole–Cole plots, weighted relaxation spectra, and elongational behavior, the low molecular weight L-PP blends with the branched PP are believed to be miscible, and the high molecular weight L-PP blends to be immiscible. The Paliene model predictions were in good agreement with the experimental data for all of the blends investigated. We considered α/R_v (i.e. the ratio of interfacial tension α to volume average radius R_v) as a fitting parameter to find the best fit of the model predictions with the experimental data. The low frequency data of a PP40/LCB-PP blend and a PP04/LCB-PP blend was well described by $\alpha/R_v=0$ and $\alpha/R_v=100$, respectively, which suggests miscibility of the PP40/LCB-PP blend and immiscibility of the PP04/LCB-PP blend. Our results confirm the finding of Fang et al. (2005) on the miscibility/immiscibility of LLDPE/LDPE blends

The applicability of the time–temperature superposition (TTS) principle was checked for the blends as well as for the neat polymers. A good validity of TTS was found for all the samples and was explained by the close values for the flow activation energy and shift factor of the samples and the small interfacial tension between the PP components.

The results from thermal analysis indicated that, a small amount of long-chain branches increases the number of nuclei sites and alternatively the degree of crystallization and rate of crystallization. By the addition of a branched polymer, a dramatic increase of the crystallization temperature was observed. Finally, it was found that the value of half crystallization time, $t_{1/2}$, decreases as the level of LCB-PP increases, indicating in that the branches behave as heterogeneous nucleating sites.

Polarized optical microscopy of the samples revealed much smaller spherulites for the blends compared to the neat linear PP. This was attributed to the combined effects of the residual catalysts and long-chain branches, indicating that these two act as nucleating agents.

A positive deviation from the Fox equation of glass transition temperature, T_g , was observed for all the blends.

Notation

a_T	thermal shift factor
G'	storage modulus, Pa
G''	loss modulus, Pa

■	matrix complex modulus, Pa
■	droplet complex modulus, Pa
H	relaxation spectrum, Pa
k	Avrami constant
M_n	number average molecular weight, kg/mol
M_w	weight average molecular weight, kg/mol
n	Avrami constant
R_v	volume average radius, μm
t	time, s
$t_{1/2}$	half time of crystallization, s
T	temperature, $^{\circ}\text{C}$
T_c	crystallization temperature, $^{\circ}\text{C}$
T_g	glass transition temperature, $^{\circ}\text{C}$
T_m	melting point, $^{\circ}\text{C}$
T_o	onset crystallization temperature, $^{\circ}\text{C}$
w	weight fraction
X	degree of crystallinity
X_c	degree of crystallinity
X_{rel}	relative crystallinity
<i>Greek letters</i>	
α	interfacial tension, alpha crystal form, mN/m
β	beta crystal form
δ	loss angle
■	strain rate, 1/s
η^*	complex viscosity, Pa s
η_o	zero-shear viscosity, Pa s
η'	real component of complex viscosity, Pa s
η''	imaginary component of complex viscosity, Pa s
■	transient elongational viscosity, Pa s
λ	relaxation time, s
μ	micron
ϕ_{β}	branched polypropylene content
Φ	cooling rate, $^{\circ}\text{C}/\text{min}$
ω	frequency, rad/s
<i>Abbreviations</i>	
DMA	dynamic mechanical analysis
DSC	differential scanning calorimetry
ETC	environmental test chamber
GPC	gas permeation chromatography
L-PP	linear polypropylene
LCB-PP	long-chain branched polypropylene
LDPE	low density polyethylene
LLDPE	linear low density polyethylene
MFR	melt flow rate
MWD	molecular weight distribution
NLREG	non linear regularization
PE	polyethylene
POM	polarized optical microscopy
PP	polypropylene
SB	sodium benzoate
TTS	time temperature superposition
WAXD	wide angle X-ray diffraction

Table options

Acknowledgement

Financial support from NSERC (Natural Science and Engineering Research Council of Canada) is gratefully acknowledged.

References

- Agarwal et al., 2003 P.K. Agarwal, R.H. Somani, W. Weng, A. Mehta, L. Yang, S. Ran, L. Liu, B. Hsiao
Shear-induced crystallization in novel long chain branched polypropylenes by in situ rheo-SAXS and -WAXD
Macromolecules, 36 (2003), pp. 5226–5235
Loading
- Ajji et al., 2003 A. Ajji, P. Sammut, M.A. Huneault
Elongational rheology of LLDPE/LDPE blends
Journal of Applied Polymer and Science, 88 (2003), pp. 3070–3077
Loading
- Arroyo and Lopez-Manchado, 1997 M. Arroyo, M.A. Lopez-Manchado
Crystallization kinetics of polypropylene: II. Effect of the addition of short glass fibres
Polymer, 38 (1997), pp. 5587–5593
Loading
- Auhl et al., 2004 D. Auhl, J. Stange, H. Münstedt
Long-chain branched polypropylenes by electron beam irradiation and their rheological properties
Macromolecules, 37 (2004), pp. 9465–9472
Loading
- Boileau et al., 2001 S. Boileau, L. Bouteiller, E. Foucat, N. Lacoudre
Stable low molecular weight glasses based on mixtures of bisphenol A and bispyridines
Journal of Material Chemistry, 12 (2001), pp. 195–199
Loading
- Bousmina and Muller, 1993 M. Bousmina, R. Muller
Linear viscoelasticity in the melt of impact PMMA. Influence of concentration and aggregation of dispersed rubber particles
Journal of Rheology, 37 (1993), pp. 663–679
Loading
- Chun et al., 2000 Y.S. Chun, Y.J. Kyung, H.C. Jung, W.N. Kim
Thermal and rheological properties of poly(ϵ -caprolactone) and polystyrene blends
Polymer, 41 (2000), pp. 8729–8733
Loading
- Dong et al., 2008 M. Dong, Z. Guo, Z. Su, J. Yu
Study of the crystallization behaviors of isotactic polypropylene with sodium benzoate as a specific versatile nucleating agent
Journal of Polymer Engineering and Science Part B Polymer Physics, 46 (2008), pp. 1183–1192
Loading
- Fang et al., 2005 Y. Fang, P.J. Carreau, P.G. Lafleur
Thermal and rheological properties of mLLDPE/LDPE blends
Polymer Engineering and Science, 45 (2005), pp. 1254–1264
Loading
- Fang et al., 2008 Y. Fang, F. Sadeghi, G. Fleuret, P.J. Carreau
Properties of blends of linear and branched polypropylenes in film blowing
Canadian Journal of Chemical Engineering, 86 (2008), pp. 6–14
Loading
- Fujiyama and Inata, 2002 M. Fujiyama, H. Inata
Rheological properties of metallocene isotactic polypropylenes
Journal of Applied Polymer and Science, 84 (2002), pp. 2157–2170
Loading
- Gotsis et al., 2004 A.D. Gotsis, B.L.F. Zeevenhoven, A.H. Hogt
The effect of long chain branching on the processability of polypropylene in thermoforming
Polymer Engineering and Science, 44 (2004), pp. 973–982

Loading

[Guan et al., 2003](#) Y. Guan, S.Z. Wang, A.N. Zheng, H.N. Xiao**Crystallization behaviors of polypropylene and functional polypropylene**

Journal of Applied Polymer and Science, 88 (2003), pp. 872–877

Loading

[Ho et al., 2002](#) K. Ho, L. Kale, S. Montgomery**Melt strength of linear low-density polyethylene/low-density polyethylene blend**

Journal of Applied Polymer and Science, 85 (2002), pp. 1408–1418

Loading

[Honerkamp and Weese, 1993](#) J. Honerkamp, J. Weese**A non linear regularization method for the calculation of relaxation spectra**

Rheologica Acta, 32 (1993), pp. 65–73

Loading

[Hussein and Williams, 2001](#) I.A. Hussein, M.C. Williams**Rheological study of the miscibility of LLDPE/LDPE blends and the influence of Tmix**

Polymer Engineering and Science, 41 (2001), pp. 696–701

Loading

[Hussein and Williams, 2004](#) I.A. Hussein, M.C. Williams**Rheological study of the influence of branch content on the miscibility of octene m-LLDPE and ZN-LLDPE in LDPE**

Polymer Engineering and Science, 44 (2004), pp. 660–672

Loading

[Jang et al., 2001](#) G.S. Jang, W.J. Cho, C.S. Ha**Crystallization behavior of polypropylene with and without sodium benzoate as a nucleating agent**

Journal of Polymer Engineering and Science Part B Polymer Physics, 39 (2001), pp. 1001–1016

Loading

[Kwang et al., 2000](#) H. Kwang, D. Rana, K. Cho, J. Rhee, T. Woo, B.H. Lee, S. Choe**Binary blends of metallocene polyethylene with conventional polyolefins: rheological and morphological properties**

Polymer Engineering and Science, 40 (2000), pp. 1672–1681

Loading

[Liu et al., 2002](#) C. Liu, J. Wang, J. He**Rheological and thermal properties of m-LLDPE blends with m-HDPE and LDPE blends**

Polymer, 43 (2002), pp. 3811–3818

Loading

[Lohse et al., 2002](#) D.J. Lohse, S.T. Milner, L.J. Fetters, M. Xenidou, N. Hadjichristis, R.A. Mendelson, C.A. Garcia-Franco, M.K. Lyon**Well-defined, model long chain branched polyethylenes. 2. Melt rheological behavior**

Macromolecules, 35 (2002), pp. 3066–3075

Loading

[Macaubas and Demarquette, 2002](#) P.H.P. Macaubas, N.R. Demarquette**Time–temperature superposition principle applicability for blends formed of immiscible polymers**

Polymer Engineering and Science, 42 (2002), pp. 1509–1519

Loading

[McCallum et al., 2007](#) T.J. McCallum, M. Kontopoulou, C.P. Park, E.B. Muliawan, S.G. Hatzikiriakos**The rheological and physical properties of linear and branched polypropylene blends**

Polymer Engineering and Science, 47 (2007), pp. 1133–1140

Loading

[Münstedt et al., 1998](#) H. Münstedt, S. Kurzbeck, L. Egersdörfer**Influence of molecular structure on rheological properties of polyethylenes. Part II. Elongational behaviour**

Rheologica Acta, 37 (1998), pp. 21–29

Loading

[Palieme, 1990](#) J.F. Palieme

Linear rheology of viscoelastic emulsions with interfacial tension

Rheologica Acta, 29 (1990), pp. 204–214

Loading

[Stange et al., 2005](#) J. Stange, C. Uhl, H. Münstedt**Rheological behavior of blends from a linear and a long-chain branched polypropylene**

Journal of Rheology, 49 (2005), pp. 1059–1079

Loading

[Stange and Münstedt, 2006](#) J. Stange, H. Münstedt**Rheological properties and foaming behavior of polypropylenes with different molecular structure**

Journal of Rheology, 50 (2006), pp. 907–923

Loading

[Steffl, 2004](#) Steffl, T. 2004. Rheological and film blowing properties of various low density polyethylenes and their blends. Dissertation, University Erlangen-Nuremberg.

Loading

[Tian et al., 2006a](#) J. Tian, W. Yu, C. Zhou**The preparation and rheology characterization of long chain branching polypropylene**

Polymer, 47 (2006), pp. 7962–7969

Loading

[Tian et al., 2006b](#) J. Tian, W. Yu, C. Zhou**Crystallization kinetics of linear and long-chain branched polypropylene**

Journal of Macromolecular Science Part B Physics, 45 (2006), pp. 969–985

Loading

[Tian et al., 2007](#) J. Tian, W. Yu, C. Zhou**Crystallization behavior of linear and long chain branched polypropylene**

Journal of Applied Polymer and Science, 104 (2007), pp. 3592–3600

Loading

[Utracki and Schlund, 1987](#) L.A. Utracki, B. Schlund**Linear low density polyethylene and their blends: Part 4 shear flow of LLDPE blends with LLDPE and LDPE**

Polymer Engineering and Science, 27 (1987), pp. 1512–1522

Loading

[Utracki, 1991](#) L.A. Utracki**Two Phase Polymer Systems**

Hanser Publisher, New York (1991)

Loading

[van Gorp and Palmen, 1998](#) M. van Gorp, J. Palmen**Time–temperature superposition for polymeric blends**

Rheology Bulletin, 67 (1998), pp. 5–8

Loading

[Wagner et al., 2000](#) M.H. Wagner, H. Bastian, P. Hachmann, J. Meissner, S. Kurzbeck, H. Münstedt, F. Langouche**The strain hardening behaviour of linear and long-chain-branched polyolefin melts in extensional flows**

Rheologica Acta, 39 (2000), pp. 97–109

Loading

[Wagner et al., 2004](#) M.H. Wagner, S. Kheirandish, M. Yamaguchi**Quantitative analysis of melt elongational behavior of LLDPE/LDPE blends**

Rheologica Acta, 44 (2004), pp. 198–218

Loading

[Wood-Adams et al., 2000](#) P.M. Wood-Adams, J.M. Dealy, A.W. Groot, O.D. Redwine**Effect of molecular structure on the linear viscoelastic behavior of polyethylene**

Macromolecules, 33 (2000), pp. 7489–7499

Loading

[Zhang et al., 2007](#) R.H. Zhang, D. Shi, S.C. Tjong, R.K.Y. Li**Study on the transformation of polypropylene crystals in compatibilized blend of**

polypropylene/ polyamide-6

Journal of Polymer Engineering and Science Part B Polymer Physics, 45 (2007), pp. 2674–2681

Loading

[Zhu et al., 2006](#) P. Zhu, J. Tung, A. Phillips, G. Edward**Morphological development of oriented isotactic polypropylene in the presence of a nucleating agent**

Macromolecules, 39 (2006), pp. 1821–1831

Loading

Corresponding author. Tel.: +1 514 340 4711x4924; fax: +1 514 340 2994.

Crown copyright © 2009 Published by Elsevier Ltd. All rights reserved.

[About ScienceDirect](#)[Contact and support](#)[Terms and conditions](#)[Privacy policy](#)

Copyright © 2016 Elsevier B.V. or its licensors or contributors. ScienceDirect® is a registered trademark of Elsevier B.V.

Cookies are used by this site. To decline or learn more, visit our [Cookies](#) page.[Switch to Mobile Site](#)

This article belongs to a special issue

[Morton Denn Festschrift](#)

Edited By Arup K. Chakraborty and Teh C. Ho

Other articles from this special issue

[Preface](#)Teh C. Ho, Arup K. Chakraborty [more](#)[Measurement of velocity and density profiles in dis...](#)Michael Gentzler, Gabriel I Tardos [more](#)[Oxygen consumption and diffusion in assemblages ...](#)Amy S. Johnson, Robert J. Fisher, Gordon C. Weir,... [more](#)[View more articles »](#)

Recommended articles

Citing articles (31)

Related book content

